



The Crime Scene Tools Identification Algorithm Based on GVF-Harris-SIFT and KNN

Nan Pan¹, Dilin Pan², Yi Liu²

¹Faculty of Civil Aviation and Aeronautical, Kunming University of Science & Technology, Kunming 650500, P.R. China

²Kunming SNLab Tech Co., Ltd., Kunming 650228, P.R. China

ABSTRACT

In order to solve the cutting tools classification problem, a crime tool identification algorithm based on GVF-Harris-SIFT and KNN is put forward. The proposed algorithm uses a gradient vector to smooth the gradient field of the image, and then uses the Harris angle detection algorithm to detect the tool angle. After that, the descriptors of the eigenvectors in corresponding feature points were using SIFT to obtained. Finally, the KNN machine learning algorithms is employed to for classification and recognition. The experimental results of the comparison of the cutting tools show the accuracy and reliability of the algorithm.

KEY WORDS: Gradient vector flow, Harris corner detection, SIFT, KNN.

1 INTRODUCTION

AFTER committing a crime, criminals tend to leave their tools in the vicinity of the crime scene. Investigators need to make a fast decision to identify and confirm the types of tools used. Meanwhile, investigators also need to judge and match the suspected crime tools recovered at the suspect's home based on the crime scene.

Traditionally, tools for committing crimes are identified by a visual inspection of images from the crime scene. This is inefficient and low in precision, and tends to cause mistakes.

Many scholars at home and abroad have made new attempts at fast object recognition from images: In foreign countries, V.G. Volostnikov et al. (2013) have proposed a new method for profile image handling based on a spiral beam. The algorithm is used to compare profiles and to identify factors determining whether two profiles are similar or proportional to each other. S.W. Hong et al. (2012) have proposed a method to detect automatically and identity flowers through colours and edge profiles. This solved the problem of image recognition failure by local recognition and establishing an image restoration

shooting angle as a result of light. K. Yamano et al. (2007) have proposed a method to extract multivalued image profiles with a Laplace Gaussian filter, using a three-valued L-G filter or five-valued panchromatic extraction method to extract image profiles. A. Chonbodeechalermroong et al. (2015) have proposed a position-classification-based local profile matching algorithm. This local profile matching algorithm is used in gesture recognition in the communications field. J. Kong et al. (2003) have proposed a neural-network-based gun recognition system based on a Self Organizing Feature Map (SOFM)-based gun recognition system neural network, and a strategy with high performance and stability based on the integration of a self-organizing network and determination. The approaches described above have accomplished the identification and tracking of crime tools to a certain extent, but several problems still remain:

1) Using two-dimensional images as sample data for comparison requires highly precise camera devices. Disagreements between reflection of light, shooting angle, and focus will directly lead to distortions of the original data, thus affecting further data analysis.

2) Restrictions set for the signal and image processing algorithms are ideal. Thus, their usefulness will be limited to matching up complex and uncertain crime tools found at the crime scene.

The current standard SIFT algorithm, with scale, rotation, light and other features invariance, has a wide range of applications in the field of object recognition. However, its feature points focus on small local details (small-scaled feature points). Crime tools of the same class are similar to this algorithm only with regard to the profile. More small-scaled feature points may seriously interfere with image similarity calculations. Thus, the standard SIFT algorithm is invalid for classifying crime tools.

For the actual crime tool image recognition and traceability requirements, due to the current signal has a more mature alignment algorithm, the similarity between the signal comparison is no longer the ultimate goal of the study. The goal here is to improve the accuracy of the image matching the contrast in the interference signal.

For the aforementioned problems, a fast crime tool tracing technology based on an improved SIFT and KNN is proposed. This technology first smoothens the image gradient field through a gradient vector flow (GVF). Shortly thereafter, the technology detects angular points of the tool by using a Harris angular point detection algorithm. Then, it obtains feature vectors corresponding to feature points by using SIFT descriptors. Finally, the technology uses a KNN algorithm for a vote decision with feature values as the sample base. In the end, this technology is proven to be usable and effective through an experiment in which the similarity degree of multiple-sample data from actual crime tool images is compared.

2 IMAGE PRE-PROCESSING

THE image taken is a triple-channel color picture, as shown in Figure 1(a) below. It is characterized by a white background, uniform illumination, high resolution, fixed shooting angle, etc. In the image to the sides, there are two angle squares with sides perpendicular to one another, and a distinct contrast between the squares and the image background.

In accordance with established practice, the upper-left angular point of the image is taken as the origin, with the x-axis in the horizontal direction and the y-axis in the vertical direction to construct a Cartesian coordinate system. Since the profile of tool is taken as the focus, its color and texture are not taken as a basis for classification. Convert the color image into a gray image using Formula (1), as shown in Figure 1(b).



Figure 1(a). Partial view of the destroy clamp

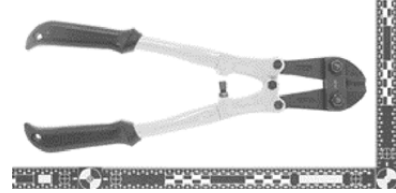


Figure 1(b). Gray image obtained by the color image

One can see that the conversion mode retains a substantial amount of contrast information of the image. Each pixel is divided by 1000 to keep the pixel value below 1.0 in order to facilitate subsequent calculations.

$$gray = 0.27 \times red + 0.71 \times green + 0.07 \times blue \quad (1)$$

2.1 Cropping the ruler

Since there may be angle squares (rulers) on both sides of the actual crime tool image at the crime scene, angle squares (rulers) are cut off based on the image edge operators, as shown below. We calculate the horizontal edge and vertical edge of image $I(x, y)$ separately:

$$Pr\ ewitt_{horizontal} = \begin{bmatrix} 1 & 1 & 1 \\ 0 & 0 & 0 \\ 1 & 1 & 1 \end{bmatrix} \quad (2)$$

$$Pr\ ewitt_{vertical} = \begin{bmatrix} 1 & 0 & 1 \\ 1 & 0 & 1 \\ 1 & 0 & 1 \end{bmatrix} \quad (3)$$

Now we turn this into an edge map $Edge(x, y)$ based on the computational process shown below:

$$Edge_{horizontal}(x, y) = Pr\ ewitt_{horizontal} * I(x, y) \quad (4)$$

$$Edge_{vertical}(x, y) = Pr\ ewitt_{vertical} * I(x, y) \quad (5)$$

$$Edge(x, y) = \sqrt{Edge_{horizontal}(x, y)^2 + Edge_{vertical}(x, y)^2} \quad (6)$$

Finally, we obtain an edge map $Edge(x, y)$ as shown in Figure 2(a).

$$EdgeSum_{horizontal}(x) = \sum_y Edge(x, y) \quad (7)$$

$$EdgeSum_{vertical}(y) = \sum_x Edge(x, y) \quad (8)$$

$$CrosshairMembership(x, y) = EdgeSum_{horizontal}(x) + EdgeSum_{vertical}(y) \quad (9)$$

$CrosshairMembership(x, y)$ represents the accumulation of strength in two orthogonal directions in the edge image $Edge(x, y)$, indicating the membership degree of the angle squares. Orthogonal lines divide the image into four areas, where the largest one is of concern. The image is as shown below in Figure 2(b) after cropping.

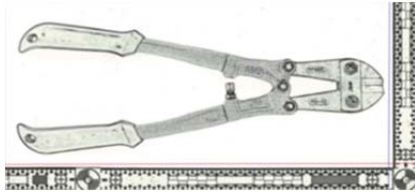


Figure 2(a). Image edge map with square tool



Figure 2(b). Tool image after cropping the ruler

2.2 Gradient Vector Flow (GVF)

In contrast to object recognition, the classification of crime tools takes no small-scaled feature points into account, so a Gradient Vector Flow (GVF) that is commonly applied to a Snake algorithm pre-treatment is introduced. GVF can obtain a smoother approximate gradient field. In this paper, GVF is used to filter some details that have small noises and sizes. For GVF, first define $f(x, y)$:

$$f(x, y) = -|\nabla I(x, y)|^2 \quad (10)$$

$$f(x, y) = I(x, y) \quad (11)$$

Define vector field $V(x, y) = (u(x, y), v(x, y))$ to be the GVF field that minimizes the energy function below:

$$\varepsilon = \iint \mu(u_x^2 + u_y^2 + v_x^2 + v_y^2) + |\nabla f|^2 |V - \nabla f|^2 dx dy \quad (12)$$

This formula may enable places lacking data to be smooth. When $|\nabla f|$ is small, the energy is dominated by the partial differential of the first part of vector field V and produces a smooth field. On the other hand, when $|\nabla f|$ is large, the second part determines the integral results. If $V = \nabla f$, the integral result is the smallest. μ is a regular parameter used to measure the contributions of the two parts of the energy function. This parameter is related to the image noise: the more noise, the larger μ is, and the GVF field V produced by a larger μ is smoother. According to the calculus of variations introduced by mathematical physics, GVF may be obtained by the following Euler equation:

$$\mu \nabla^2 u - (u - f_x)(f_x^2 + f_y^2) = 0 \quad (13)$$

$$\mu \nabla^2 v - (v - f_y)(f_x^2 + f_y^2) = 0 \quad (14)$$

When f is homogeneous, the second parts of Formulas (13) and (14) is zero, and u and v are determined separately by the Laplace equation. Figures 3(a) and Figures 3(b) show the results of a female image gradient field after being processed by GVF. The blank region in Figures 3(a) is filled, and its vector field becomes smoother.

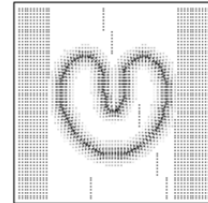


Figure 3(a). Gradient field of female image

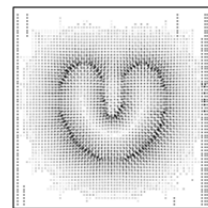


Figure 3(b). GVF field of female image

Solutions to Formulas (13) and (14) can be obtained by the following iterative:

$$u_{n+1} = \mu \nabla^2 u_n - (u_n - f_x)(f_x^2 + f_y^2) \quad (15)$$

$$v_{n+1} = \mu \nabla^2 v_n - (v_n - f_y) (f_x^2 + f_y^2) \quad (16)$$

When n is large enough, GVF tends toward stability, and this GVF is the GVF field to be solved. In this paper, $m=0.1$, $n=50$, and $f = I(x, y)$ is employed to determine the strength of the GVF field, as shown in Figure 4(b). The strength of the original GVF field is shown in Figure 4(a). In Figure 4(b), the noise gradient strength is under effective suppression, and the tool profile is expanded. Obviously, GVF is in favor of improving smooth gradients and packing uniform area gradients. After that, the noise reduction effect has been improved, the accuracy and speed of image processing has been greatly enhanced.



Figure 4(a). Gradient field strength of image

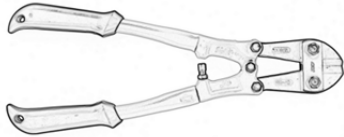


Figure 4(b). GVF field strength of image

3 FEATURE DETECTION AND QUANTIFICATION

IN this paper, the angular point detection algorithm is used to determine the structure tensor on pixels of the gray image $I(x, y)$.

$$H = \begin{bmatrix} I_x^2 & I_x I_y \\ I_x I_y & I_y^2 \end{bmatrix} \quad (17)$$

Matrix H is the Harris matrix. Because the angular point has a significant change in any direction, the corresponding Harris matrix has two large eigenvalues λ_1 and λ_2 subject to eigenvalue decomposition. Similarly, one can easily determine the following rules:

When $\lambda_1 \approx 0$ and $\lambda_2 \approx 0$, there are no valuable traits;

When $\lambda_1 \approx 0$ and λ_2 has a large positive value, it indicates that an edge has been detected;

When both λ_1 and λ_2 have large positive values, it indicates that an angular point has been detected.

However, H may greatly enlarge existing small noise because H is a Harris matrix in essence (i.e., a matrix after second-order differentiation). In this paper, the way to obtain the Harris matrix is improved, and after normalization of each gradient of the obtained GVF field V , one can get $V_{normalize} = (s(x, y), t(x, y))$. In order to eliminate the influence of the strength of field V , an improved Harris matrix is obtained through a differential operation, as shown in Formula 18:

$$H_{GVF} = \begin{bmatrix} s_x & s_y \\ t_x & t_y \end{bmatrix} \quad (18)$$

Use the following formula to calculate the membership degree M_c of the Harris angular point detection:

$$M_c = \lambda_1 \lambda_2 - \kappa (\lambda_1 + \lambda_2)^2 = \det(H_{GVF}) - \kappa \text{trace}^2(H_{GVF}) \quad (19)$$

According to Formula (19), the determinant of H_{GVF} can be calculated to efficiently obtain M_c , where κ is set between 0.04–0.15.

After obtaining the corner membership, set the appropriate threshold and eliminate all thresholds that are less than the threshold. Angular points can be found at the corner of the image. If these points are completely regarded as feature points, the information will lead to redundancy. In this paper, we screen feature points using a method similar to SIFT: we choose the extreme value point in the field. If a feature point is the largest point in a field, the point can be used as a feature point and the other point is eliminated.

Figure 5(a) shows the distribution map of the final key points. After a comparison, it is found that the feature points in Figure 9 are distributed mostly at the corner positions and receive no angular point detection of GVF, as shown in Figure 5(b). There are many noise points, and it is impossible to separate the expected feature points from these disturbance points by raising the threshold.



Figure 5(a). Feature points with GVF detection



Figure 5(b). Feature points without GVF detection

4 KNN CALCULATION

FOR KNN calculation, it is required to input samples to be tested and compare them with all correctly classified samples to calculate their difference. Since the samples are expressed by vectors between 0 and 1, two vectors can be put together by logical addition (xor) and their mean can be solved. A smaller mean indicates a smaller difference and a higher degree of similarity between the two vectors. The concrete calculation formula is as follows:

$$d_{ab_k} = \frac{\sum_{i=0}^n (a_i \text{ xor } b_{ki})}{n} \quad (20)$$

where a is the vector the sample to be tested, b_k is the number k correctly classified sample for main internal comparison, n is the number of dimensions of the vector, a_i represents the number-i feature value of a, and b_{ki} is calculated in a similar way. d_{ab_k} is the distance between the final two vectors.

In addition to the distance calculation formula, the rest should follow the steps of the KNN algorithm, the calculated distance value should be saved in a specific location.

Most often, KNN chooses K (the industry standard of three) nearest samples to vote on the class to which each sample belongs, then chooses the most-voted class for output. Generally, there are two voting patterns: simple voting and weighted voting.

5 EXPERIMENTAL VERIFICATION

SIMPLE voting: majority vote rules. Take the class that has the most midpoints in the neighborhood.

In order to validate the technique presented in this paper using actual crime image similarity matching results, experiments are performed to verify its feasibility. In order to make the experimental data sufficient, a variety of tools have been experimentally verified.

The sample coding rule used in the experiment is G-Xa. G is a fixed value, and X is the tool serial number used to distinguish between different tool sample groups (for example, GA represents the first class of tools, and GB represents the second class). When a = 0, it represents samples to be tested. When a=1-4, it represents four different shooting angles of the same image in the sample library.

Images are taken by mainstream phones with an f/2.0 lens and 13 million pixels. The image matching program is written in Eclipse + Java + OpenCV. All tool images are taken by the same phone. The matching program runs on a Macbook Pro with an Intel Core i5 2.9 GHz (CPU) and 8-GB DDR3.

Weighted voting: According to the distance, add weight of closer votes. For example, if the distance is shorter, then the weight is larger. (Weight is the inverse square of the distance).

In this algorithm, weighted voting is adopted with a weight of $1 - distance$. Weighted voting not only has higher accuracy but also a more stable performance with higher efficiency compared with simple voting.

After voting, the method that outputs the highest number of votes is taken as the most similar result.

Images of a total of 10 cutting tools commonly used for committing a crime (wire clipper, destroy plier, vise, hydraulic clamp, etc.) are selected for test many times. A total of 10 groups of signal features to be tested are obtained. In the sample library, there are 210 groups of sample detection signal features (including 10 groups of sample data above to be tested) contributed by images of 50 types of crime tools taken from four different angles. Specific sample codes to be tested are listed in Table 1.

Table 1. Coding of samples to be tested

Sample code	Tool No
G-A0	A
G-B0	B
G-C0	C
G-D0	D
G-E0	E
G-F0	F
G-G0	G
G-H0	H
G-I0	I
G-J0	J

During the test, first eliminate the data that are exactly the same. Define criteria of identification based on the test results:

- 1) Samples where the same tool fails to be identified are defined to be a non-mismatch.
- 2) Samples at one or more angles where the same tool is identified are defined to be a match.

In order to ensure repeatability and robustness of the algorithm used in the tests, each sample is subject to 10 similarity matching tests, and the samples with the highest matching degree are taken as the most similar ones. Ten groups of data are given a total of 100 tests. The results are as listed in Table 2. Sample matching takes nearly 2 s. The samples with the highest matching degree are selected as matching results. There are only two false matches at a match rate of approximately 98%.

Table2. Sample matching results using proposed algorithm

Sample to be tested	Sample with the highest matching degree	Matches`	False match
G-A0	G-A1	100%	0%
G-B0	G-B1	100%	0%
G-C0	G-C3	100%	0%
G-D0	G-D2	90%	10%
G-E0	G-E1	100%	0%
G-F0	G-F4	100%	0%
G-G0	G-G2	90%	10%
G-H0	G-H1	100%	0%
G-I0	G-I1	100%	0%
G-J0	G-J4	100%	0%

A multisource remote sensing image registration algorithm based on composite transformation presented by algorithm which Y.Z. Li et.al (2014) proposed is compared with the technology proposed in this paper. We solve the global geometric difference between images by using a gray transform to extract stable structure features between optical and SAR images. Weight is added to algorithm based on a log-polar transformation. In the end, a series of match points are obtained through a local geometry transform to realize image registration. A total of 100 tests are conducted for 10 groups of data. The results are listed in Table 3. Sample matching takes nearly 3 min. The samples with the highest matching degree are selected as matching results. There are 49 false matches at a match rate of approximately 51%.

Table4. Sample matching results using algorithm which Y.Z. Li et.al (2014) proposed

Sample to be tested	Sample with the highest matching degree	Matches	False match
G-A0	G-A2	70%	30%
G-B0	Other	40%	60%
G-C0	G-C4	60%	40%
G-D0	Other	0%	100%
G-E0	G-E1	70%	30%
G-F0	G-F4	70%	30%
G-G0	G-G2	80%	20%
G-H0	Other	20%	80%
G-I0	G-I3	40%	60%
G-J0	G-J4	60%	40%

Thus, it can be seen that the algorithm presented by Y.Z. Li et.al (2014) has disadvantages such as low accuracy, inefficiency, and poor stability in matching and identifying large numbers of crime tool image data. By contrast, the algorithm proposed in this article enjoys obvious advantages by several orders of magnitude in its operation accuracy, stability, and efficiency. The iterative process of this algorithm is not complicated, and also easy to program using high-level programming languages such as Java. Thus, the proposed algorithm offers higher practical engineering value in tracing and matching the actual crime tool image data.

6 CONCLUSION

AS proven by actual crime tool feature comparison tests, the concepts in this paper smooth the image gradient field through a gradient vector flow (GVF), then detects angular points of the tool by using a Harris angular point detection algorithm. Next, we obtain features vectors that feature points that correspond by using SIFT descriptors. Finally, we use a KNN algorithm for vote decision with feature values as the sample base. This technology makes it possible to effectively extract crime tool profile features, transform them into feature vectors, and apply them to the adaptive matching of crime tools.

According to the actual investigation of many criminal tools research experts of the public security organs, this technology is effective for comparing and matching the images of the crime tools effectively, which provides a reliable basis for the quick tracing of the criminal tools. The following subjects require further study: how to introduce fast dynamic time adjustment, machine learning, and other advanced tool tracing algorithms to further simplify the matching operation, and improving the data calculation speed by higher orders of magnitude.

7 ACKNOWLEDGMENT

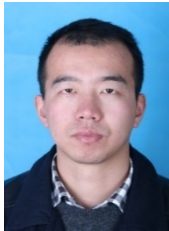
THIS article was supported by the key project of technology research program funded by Yunnan Province (approved grants 2016RA042), the Innovation Fund for Technology based firms in Yunnan Province (approved grants 2014SC030 and 2017EH028), the key science and technology project of Kunming City (approved grants 2015-1-S-00284), the Ministry of public security technology research program (approved grants 2014JSYJA020 and 2016JSYJA03).

8 REFERENCES

- A. Chonbodeechalermroong, T.H. Chalidabhongse, (2015). Dynamic contour matching for hand gesture recognition from monocular image. *Institute of Electrical and Electronics Engineers Inc*, 47-51.
- G. Hermosilla, J. Ruiz-Del-Solar, R. Verschae, (2017). An enhanced representation of thermal faces for improving local appearance-based face recognition. *Intelligent Automation and Soft Computing*, 23(1):1-12.
- S.W. Hong, L. Choi, (2012). Automatic recognition of flowers through color and edge based contour detection. *IEEE Computer Society*, 141-146.
- J. Kong, D.G. Li, A.C. Watson, (2003). A firearm identification system based on neural network. *Conference on Ai: Advances in Artificial Intellig*, Springer Verlag, 315-326.
- Y.Z. Li, J. Zhang, (2014). New intrusion detection algorithm based on cluster and cloud model.

- Journal of Electronic Measurement and Instrument*, 28(12): 1376-1381.
- C.Y. Park, M.S. Lee, Y.S. Kim, et.al, (2018). Sensor data abstraction for failure prediction of polymerase chain reaction thermal cyclers. *International Journal of Engineering and Technology Innovation*, 8(3): 191-199.
- V. G. Volostnikov, S. A. Kishkin, S. P. Kotova, (2013). "New method of contour image processing based on the formalism of spiral light beams". *Turpion Ltd., Blackhorse Road*, 43(7): 646-650.
- K. Yamano, C.K .Pham, Takanori, (2007). Multiple-valued image-contour extraction method using a Laplacian-Gaussian filter. *John Wiley and Sons Inc*, 38(8):61-71.

9 NOTES ON CONTRIBUTORS



Nan Pan, from Huaiyuan, Anhui Province, Ph.D., Master Instructor, received Ph.D. degree in 2012 from Kunming University of Science & Technology. Now, he is an associate professor in Faculty of Civil Aviation and Aeronautical, Kunming University of Science & Technology. His main research

directions include signal processing, forensic science equipment R&D.

E-mail: 15808867407@163.com



Dilin Pan, from Huaiyuan, Anhui Province, Professor, Master Instructor, received B.Sc. degree in 1982 and received Master degree in 1986 from Anhui University of Science & Technology respectively. Now, he is the chief engineer of Kunming SNLab Technology Co. Ltd.. His main research directions include signal processing, forensic science equipment R&D.

E-mail: dilinpan@camsonar.com



Yi Liu, from Leshan, Sichuan Province, graduated from Baicheng Normal University in 1998. Now, he is the general manager of Kunming SNLab Technology Co. Ltd. His main research direction includes forensic science equipment R&D.

E-mail: yiliu@camsonar.com